Climate Sensitivity of a One-Dimensional Radiative-Convective Model with Cloud Feedback

WEI-CHYUNG WANG[1]

Atmospheric and Environmental Research, Inc., Cambridge, MA 02139

WILLIAM B. ROSSOW AND MAO-SUNG YAO

NASA Goddard Institute for Space Studies, New York, NY 10025

MARILYN WOLFSON[2]

Department of Meteorology and Physical Oceanography, MIT, Cambridge, MA 02139

(Manuscript received 27 July 1980, in final form 9 February 1981)

ABSTRACT

We illustrate the potential complexity of the feedback between global mean cloud amount and global mean surface temperature when variations of the vertical cloud distribution are included by studying the behavior of a one-dimensional radiative-convective model with two types of cloud variation: 1) variable cloud cover with constant optical thickness and 2) variable optical thickness with constant cloud cover. The variable parameter is calculated assuming a correlation between cloud amount and precipitation or the vertical flux convergence of latent heat. Since the vertical latent heat flux is taken to be a fraction of the total heat flux, modeled by convective adjustment, we examine the sensitivity of the results to two different critical lapse rates, a constant 6.5 K km^{-1} lapse rate and a temperature-dependent, moist adiabatic lapse rate. The effects of the vertical structure of climate perturbations on the nature of the cloud feedback are examined using two cases: a 2% increase in the solar constant and a doubling of the atmospheric carbon dioxide concentration. The model results show that changes in the vertical cloud distribution and mean cloud optical thickness can be as important to climate variations as are changes in the total cloud cover. Further the variety and complexity of the feedbacks exhibited even by this simple model suggest that proper determination of cloud feedbacks must include the effects of varying vertical distribution.

1. Introduction

The sensitivity of the earth's atmospheric radiation budget to *specified* changes in total cloud cover and in mean cloud top altitude has been demonstrated in many models (Manabe and Wetherald, 1967; Cox, 1971; Schneider, 1972; Fleming and Cox, 1974; Cess, 1974; Lacis *et al.*, 1979; Stephens and Webster, 1979); but, since clouds vary in response to changes in the atmospheric state, a key problem in understanding the behavior of earth's climate is to determine the nature of cloud-radiation *feedbacks*. Previous studies of cloud feedback have considered only those produced by changes in the areal coverage of a single cloud layer, effectively, with specific optical properties[3] (Paltridge, 1974; Temkin *et al.*, 1975; Petukhov *et al.*, 1975; Gates, 1976; Roads, 1978; Schneider *et al.*, 1978) and by a simple kind of cloud altitude change which maintains a fixed cloud temperature (Cess, 1974, 1976; Wang and Stone, 1980). However, model studies with specified cloud changes show that the *net* radiative effect of a cloud-cover change depends on the altitude of the cloud top and that the behavior of cirrus clouds is especially sensitive to variations of their optical thickness (see especially, Stephens and Webster, 1979). Both of these factors have been neglected in previous feedback studies. Furthermore, the altitude dependence of the cloud radiative effects suggests that complete understanding of cloud feedbacks requires understanding the role of variations in the vertical distribution of cloud properties and their interaction with the vertical structure of the climate perturbations themselves.

The mean vertical distribution of some cloud properties is known in broad outline, but large uncertainties exist in our knowledge of high-level clouds, of clouds over oceans, and of the diurnal and seasonal variability of clouds in general (see, e.g., GARP, 1975; Oxford, 1978). Furthermore, we know little about the complex of processes that

[1] Work completed while author was at NASA Goddard Institute for Space Studies in New York.

[2] Author contributed to this research while participating in the Summer Institute on Planets and Climate at the Goddard Space Institute for Space Studies and Columbia University.

[3] Wetherald and Manabe (1980) recently have considered a model with multiple cloud layers.

0022-4928/81/061167-12$07.00

TABLE 1. Cloud cover and optical thickness as a function of altitude obtained in the model when adjusted to the current climate using a constant, 6.5 K km^{-1}, lapse rate and a temperature-dependent, moist adiabatic lapse rate as the critical lapse rate in the convective adjustment scheme.

	Fixed lapse rate		Moist adiabatic lapse rate	
Altitude (km)	Cloud cover (%)	Optical thickness	Cloud cover (%)	Optical thickness
12	0	0	0	0
9	2.4	2.10	0	0
8	5.6	1.83	2.3	3.22
5	6.2	6.89	6.2	7.54
4	10.2	6.72	12.5	6.87
3	7.8	6.57	9.3	6.49
2	6.2	17.56	7.0	17.01
1	5.5	18.19	5.7	17.39
0	6.7	18.80	6.0	17.87
Total	50.6	78.65	49.0	76.39

determine the *mean* vertical distribution of clouds (see, e.g., Krishnamurti *et al.*, 1980; Webster and Stephens, 1980).

One-dimensional radiative-convective (1-D RC) models (see Ramanathan and Coakley, 1978) are particularly suited to investigation of this problem for two reasons. First, this model, as a representation of the global and annual mean atmospheric structure, isolates the mean vertical cloud distribution and the processes controlling it so that the key relationships are more easily examined. Second, the simplicity of the parameterized dynamics allows for a more detailed treatment of the radiative transfer problem so that the proper relationship between cloud visual albedo and infrared emissivity can be incorporated. This relationship is crucial for proper modeling of both the altitude dependent cloud radiative effects and the effects of cirrus clouds (Lacis *et al.*, 1979; Stephens and Webster, 1979; Stephens, 1980). The crude state of our theory and data concerning vertical cloud distributions and processes makes study of simple parameterizations in such simple models a desirable prelude to more complex model studies. The cloud parameterization that we introduce in Section 2 is simple, but it is self-consistent and retains the key feature of allowing the clouds at different altitudes to vary individually in response to changes in the vertical temperature structure and atmospheric dynamics. Although we believe that the parameterization is plausible, we intend our model results to serve primarily as an *illustration* of the *potential* complexity of the cloud feedbacks when vertical structure variations are included.

To display the dependence of the model behavior on the vertical structure of the climate perturbation, we consider two cases: a 2% increase in the solar constant (Section 3) and a doubling of the CO_2 abundance (Section 4). Without cloud feedback in this model, both of these perturbations produce about the same change in the global and annual mean surface temperature. However, since these two perturbations accomplish this surface warming in different ways, their interactions with the cloud processes lead to different feedbacks. We discuss the implications of this result and summarize our conclusions in Section 5.

2. Model

a. Basic 1-D RC model

The 1-D RC model used here is that of Wang *et al.* (1976) and represents the global and annual mean atmospheric temperature structure at equilibrium. The model equilibrium is attained by a forward time-marching computation until energy balance occurs at all altitudes. For an assumed initial atmospheric composition, global mean surface albedo and initial global mean vertical distribution of temperature and clouds, the solar and thermal flux divergences averaged over clear and cloudy fractions are computed at 17 unequally spaced altitudes covering the lowest 50 km of the atmosphere (see Table 1). The model relative humidity is fixed; thus, the absolute humidity changes with the temperature causing a significant positive temperature feedback (Manabe and Wetherald, 1967). The net radiative heating/cooling at each altitude, together with the "convective" heating/cooling discussed below, determines the atmospheric temperature at the next time step. The surface temperature at the next time step is calculated from a balance between solar, thermal and convective fluxes, where the latter is determined from stability criteria using the previous time step surface temperature and the next time step atmospheric temperature. The total convective flux convergence in the atmosphere equals the convective flux divergence in the surface energy budget.

At any level where the computed temperature lapse rate is steeper than a specified critical lapse rate, convective heating is assumed sufficient to return the temperature lapse rate to the critical value. This procedure is called convective adjustment (Manabe and Strickler, 1964). However, in addition to actual small-scale convective vertical heat fluxes, this adjustment must represent the global mean vertical heat fluxes by large-scale dynamics which are driven primarily by the equator-to-pole temperature gradient. These effects are generally represented by using a constant, empirical, critical lapse rate of 6.5 K km^{-1} (Manabe and Strickler, 1964); but Stone and Carlson (1979) show better agreement with the observed global and annual mean temperature structure using the moist

adiabatic lapse rate. Neither of these lapse rates, however, may correctly describe the lapse rate changes during climate variations. We use both a constant and a moist adiabatic lapse rate in the convective adjustment to test the sensitivity of our results to this parameterized heat flux and to *illustrate one possible temperature feedback.*

The above description applies to most current 1-D RC models (Ramanathan and Coakley, 1978), but these models differ in the methods used to solve the radiative transfer equations. We use a method that explicitly accounts for vertical inhomogeneity in atmospheric composition and aerosol distribution using the doubling and adding techniques to calculate multiple scattering effects (Lacis and Hansen, 1974) and the correlated k-distribution method of integrating over frequency (Lacis *et al.*, 1979). One advantage of this approach is that realistic spectral properties of clouds and aerosols can be employed to avoid the grey approximation (see Section 2b).

In addition to the convective adjustment and fixed relative humidity assumptions, most models have constant global mean surface albedos, and fixed aerosol and cloud distributions. Wang and Stone (1980) have studied an ice albedo-temperature feedback in a 1-D RC model, as well as variable clouds with the FCT parameterization suggested by Cess (1974). We consider here a fixed cloud altitude (FCA) model in which either *mean* cloud cover or cloud optical thickness at each model level can vary. The latter variation has not been considered previously as a source of cloud feedback.

b. Cloud properties

The cloud properties in this model are chosen so that the control experiments produce the observed global and annual mean vertical temperature structure. Hence the cloud fractional cover and optical thickness[4] in each model layer represents those properties of non-overlapping, plane-parallel clouds that interact with the radiation to produce the correct global and annual mean net radiative heating/cooling. *These clouds do not, therefore, represent the global and annual mean cloud cover and optical thickness at each level; but rather, they represent the mean cloud properties weighted by their radiative effects.* In control runs for variable cloud cover experiments, the optical thickness is fixed at $\tau = 16$ ($z < 3$ km), $\tau = 6$ ($3 \leq z < 8$ km) and $\tau = 2$ ($z \geq 8$ km). The best match to observed temperature is obtained with the cloud cover distribution shown in Table 1. In control runs for variable optical thickness experiments, the cloud cover is fixed at the values in Table 1; however, because of the different coupling to cloud liquid water content in these experiments (explained below), the best match to observed temperatures is obtained by adjusting the optical thickness distribution to that shown in Table 1.

The reflection, absorption and transmission of the clouds are calculated as a function of wavelength and optical thickness, taking full account of multiple scattering effects [see Wang *et al.* (1976) and Lacis *et al.* (1979) for details]. For these calculations the clouds are assumed composed of water spheres ($z < 8$ km) or ice spheres ($z \geq 8$ km) with a particle size distribution given by a gamma distribution (Hansen, 1971). The effective particle radius and effective variance characterizing this distribution are 10 μm and 0.15 for water clouds and 25 μm and 0.1 for ice clouds. The wavelength dependence over the solar and thermal spectra is taken from Hale and Querry (1973) for water and Irvine and Pollack (1968) for ice. In the variable optical thickness experiments, the cloud liquid water content and optical thickness are linked by assuming a particle number density of 350 cm^{-3} ($z < 3$ km), 450 cm^{-3} ($3 \leq z < 8$ km) and 5 cm^{-3} ($z \geq 8$ km) (Yamamoto *et al.*, 1971).

To illustrate the net radiative effect of a specified cloud variation, we show in Fig. 1 the change in equilibrium surface temperature produced by adding 10% cloud cover at 8 km with variable optical thickness. The reference model has 30% cloud cover at 3 km and 10% cloud cover at 5 km; both clouds are optically thick. The separate visual and thermal components of the total effect are also shown. The warming caused by the thermal effect of the cloud increases more rapidly at first with increasing optical thickness than does the cooling produced by the albedo effect, so that, in this case, it dominates for $\tau \leq 8$. The effect of cloud altitude on the results shown in Fig. 1 is given by a rough scaling of the magnitude of the thermal effect with the difference between the surface and cloud top temperature. *This altitude dependence, together with the decrease of cloud optical thickness with increasing altitude, makes possible the complicated feedbacks produced in our model by variations of the cloud vertical distribution.*

c. Cloud parameterization

The cloud parameterization that we employ in this study is inferred from the observed correlation between the large-scale horizontal distributions of cloud amount and precipitation. Although the climatologies of clouds and precipitation are not well enough known, especially over oceans, to determine how much non-precipitating cloudiness occurs

[4] Optical thickness refers to visual optical thickness throughout this paper.

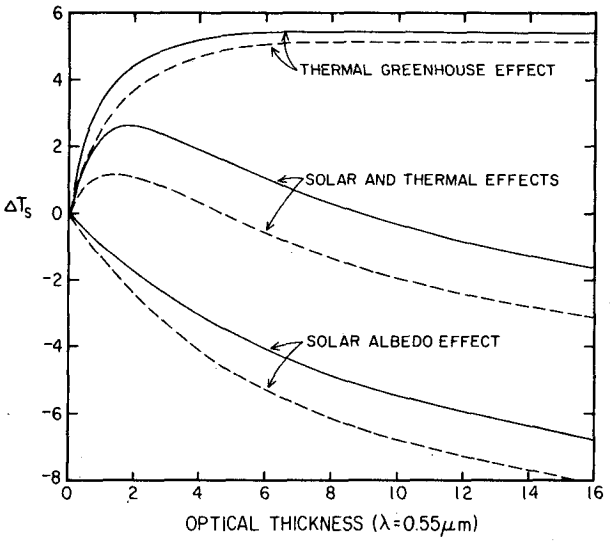

FIG. 1. Thermal greenhouse effect and solar albedo effect of ice cloud (solid line) and water cloud (dashed line, 5 μm effective particle radius) on surface temperature T_s (K). These effects are caused by the addition of 10% cloud cover at 8 km to a reference model with clouds at 3 and 5 km (see text). The net radiative effect is also shown.

(GARP, 1975), several associations between cloud systems and precipitation zones are qualitatively known:

1) Distinctive ITCZ cloud systems coincide with the zone of maximum precipitation near the equator and follow its seasonal shifts.

2) Low cloud cover regions in the subtropics coincide with the major world deserts.

3) Characteristic midlatitude clouds are associated with the frontal systems of cyclonic low pressure "storms" which produce zones of heavy precipitation along well-defined "storm tracks."

Recent analyses of GATE observations suggest that the most characteristic precipitating cloud system in the tropics is composed of a cluster of deep, precipitating cumulus towers with an associated mesoscale stratus cloud which produces a substantial fraction of the total precipitation (Johnson, 1980; Leary and Houze, 1980; Webster and Stephens, 1980). Ludlam (1980) reviews observations of midlatitude cyclones which show that the precipitation occurs primarily along the associated warm and cold fronts, falling from mesoscale complexes of cumuloform and stratoform clouds. Both tropical and extratropical systems are always accompanied by large-scale cirrus clouds. Regardless of which type of cloud produces most of the global precipitation, these observations suggest that most of the large-scale clouds which dominate the radiation budget are produced by the same mesoscale and synoptic scale systems which produce the precipitation. Very little climatological information is available regarding the vertical structure of these precipitating systems (GARP, 1975; Oxford, 1978; Krishnamurti *et al.*, 1980), but we assume that *the global and annual mean vertical cloud distribution can be related in some way to the mean vertical precipitation distribution.*

In equilibrium the precipitation rate is proportional to the latent heating rate of the atmosphere. The latent heating rate, plus the sensible heating rate, in turn, must balance the radiative cooling rate of the atmosphere. (The surface balance is radiative heating equals latent and sensible cooling.) The fact that the clouds also strongly influence the radiative heating of the surface and the cooling of the atmosphere shows the fundamental importance and potential complexity of the cloud-radiation feedback problem. In a 1-D RC model, the latent heating rate is some fraction of the total vertical heat flux convergence represented by convective adjustment. No simple or complete theory exists as yet to relate the latent heat flux to the sensible heat flux or to the cloud amount associated with synoptic and mesoscale precipitating systems; however, we propose simple, self-consistent approximations which retain some of the possible relationships. Further work on understanding cloud processes in these large, organized circulation systems, together with detailed global and seasonal cloud climatologies, is needed to determine the proper parameterization of cloud vertical distributions.

The ratio of the sensible and latent heat fluxes at the surface defines the Bowen ratio B which, therefore, represents the partitioning of the total convective cooling that balances the net radiative heating of the surface. Consequently, the global mean evaporation (or latent cooling) rate E at the surface can be expressed as

$$E = \hat{H}_l/L = \hat{H}_c[L(1 + B)]^{-1}, \qquad (1)$$

where $\hat{H}_c$ represents the vertically integrated convective heat flux convergence in the atmosphere, which is equal to the net radiative heating in the model surface energy budget, $\hat{H}_l$ is the fraction of $\hat{H}_c$ attributed to latent heating, and L is the latent heat of water condensation. In equilibrium, this evaporation rate at the surface equals the total precipitation or latent heating rate of the whole atmosphere. The conversion of total energy and water then requires that the ratio of the vertically integrated sensible and latent heating rates of the whole atmosphere equals B. We are concerned here with new equilibrium states of the model which are not very different from the initial (current) climate; hence, quantities either remain constant or vary linearly with the changing model conditions. Four simplifying assumptions allow us to use (1) to predict the mean vertical cloud distribution.

(i) The simplest assumption about the vertical de-

pendence of the ratio of the sensible and latent heating rates is that the ratio is a constant independent of altitude. The constraint mentioned above requires this constant to be B; thus, the latent heating rate per unit mass H_l at any altitude is related to the convective heating rate H_c per unit mass in the model by

$$H_l = H_c(1 + B)^{-1}. \quad (2)$$

The only global and annual mean data available to check this relationship include the vertical fluxes of latent and sensible heat by the mean meridional circulation and stationary eddies (Oort and Rasmussen, 1971). These data do show a nearly constant Bowen ratio in the lower troposphere, but the contribution of transient eddies and small-scale turbulence is unknown.

(ii) We assume that the relative humidity at each altitude level is fixed. This assumption is the simplest approximation to the increase in water vapor abundance with increasing atmospheric temperature for small changes in climate. The vertical profile of relative humidity is that of Manabe and Wetherald (1967).

(iii) Following Ogura and Takahashi (1971), we calculate the precipitation rate P from

$$P = f_1 l, \quad (3)$$

where f_1^{-1} represents a conversion time of cloud droplets into rain and l is the cloud liquid water mixing ratio at each altitude *for those cloud elements which actually contribute to the precipitation produced by the whole synoptic or mesoscale cloud system*. A value of $f_1 = 1.25 \times 10^{-4}$ s^{-1} $\sim$ (2 h)$^{-1}$ seems representative (Mason, 1971). Since the changes in l calculated for different climates are generally small, a more realistic, nonlinear parameterization (e.g., Sundqvist, 1978) is not warranted.

(iv) When the liquid water mixing ratio of the precipitating cloud elements changes, we expect the properties of the whole synoptic or mesoscale cloud system in which they are embedded to change also. *In this model the cloud cover and optical thickness do not pertain to those of an individual cloud element or even of an individual cloud system, but rather they pertain to the global and annual average properties of all synoptic and mesoscale cloud systems weighted by their radiative effects.* Our theoretical understanding and available data do not yet define a relationship between the mean cloud system properties and the mean precipitation rate, so we adopt the reasonable hypothesis that higher precipitation rates imply more vigorous cloud systems. For illustrative purposes, we assume that increased system vigor implies either larger cloud area A (model 1) or larger cloud optical thickness τ (model 2). As with precipitation we use a linear relation. Thus, for model 1 optical thickness is specified (cf. Section 2b) and

$$A = l/f_2, \quad (4)$$

where $f_2 = 5.5 \times 10^{-4}$ represents a typical mixing ratio for precipitating cloud systems (cf. Mason, 1971). For model 2, cloud cover is specified (Table 1) and

$$\tau = f_3 l, \quad (5)$$

where $f_3 = 3.09 \times 10^4$ ($z < 3$ km), 1.15×10^4 ($3 \leq z < 8$ km) and 2.75×10^3 ($z \geq 8$ km), which compares well with other models (Carrier *et al.*, 1967; Yamamoto *et al.*, 1971).

Assumptions (i) and (iii) lead to a prognostic equation for the mean liquid water mixing ratio at each altitude which contributes to precipitation:

$$\frac{\partial l}{\partial t} = H_c[L(1 + B)]^{-1} - f_1 l, \quad (6)$$

where the first term on the right is the condensation rate which is equal to the latent heating rate given by (2). This expression satisfies the constraint that, in equilibrium, the vertically integrated precipitation rate equals the global mean evaporation rate given by (1).

The second assumption leads to a simplified formula for the Bowen ratio, which is defined at the surface as

$$B = \frac{C_p}{L}[\overline{w'T'}][\overline{w'q'}]^{-1}, \quad (7)$$

where C_p is the specific heat of air and the last two factors in brackets represent the total surface fluxes of heat and moisture, respectively. The overbar indicates a horizontal and time average and the prime indicates a deviation from that average. Since the relative humidity R is fixed, the specific humidity q is proportional to the saturation specific humidity q_s, which can be expanded about a mean temperature $\bar{T}$ when $T' \ll \bar{T}$, *viz.*,

$$q_s(\bar{T} + T') = q_s(\bar{T}) + T'\frac{\partial q_s(\bar{T})}{\partial T} + \cdots. \quad (8)$$

Identifying q'/R with the second term on the right in (8), neglecting the higher order terms, and substituting into (7), we find an expression for B which is approximately equal to the empirical expression derived by Priestly and Taylor (1972):

$$B = \frac{1}{4}\frac{C_p}{RL}\left[\frac{\partial q_s(T)}{\partial T}\right]^{-1}, \quad (9)$$

where T is now taken to be the global mean surface temperature. Because of the strong temperature dependence of the factor in brackets in (9), the global mean value of B is not equal to (9) evaluated using the global mean surface temperature; therefore, we have introduced the factor (1/4) to match the observed global mean value of B (Budyko, 1956). This

expression for the Bowen ratio implies $\partial B/\partial T < 0$; that is, as the surface temperature increases, more of the surface cooling is accomplished by water evaporation.

The fourth assumption, together with Eqs. (2), (3), (6) and (9), gives the cloud cover and cloud optical thickness as a function of the total convective heat flux convergence at each altitude *in equilibrium*:

$$A = H_c[f_1 f_2 L(1 + B)]^{-1}, \tag{10}$$

$$\tau = H_c f_3[f_1 L(1 + B)]^{-1}, \tag{11}$$

respectively. Consequently, our cloud parameterization is equivalent to a fixed cloud altitude model with variable cloud properties at each level connected by the single adjustable factor in brackets (10) and (11) to the convective heat flux convergence. We have, at this stage, introduced an empirical altitude dependence of these factors through the altitude independence of f_2 and the altitude dependence of f_3, which represents the combined altitude dependence of all the factors in the brackets in a more realistic parameterization.

The expressions for the cloud cover [Eq. (10)] and cloud optical thickness [Eq. (11)] contain two contributions to the total temperature dependence of these quantities. The variation of the Bowen ratio with temperature, as discussed above, contributes a tendency for increasing cloud cover or cloud optical thickness with increasing temperature. The contribution of the convective heating factor H_c cannot be determined for all cases, however. For example, even if the total vertically integrated convective heating $\hat{H}_c$ of the atmosphere increases with increasing surface temperature, the *local* convective heating H_c at a particular altitude may either increase or decrease. The consequent local change in A or τ with increasing temperature may thus have either sign. Since the radiative effects of the clouds at different altitudes differ substantially (cf. Section 2b), the net radiative effect of cloud changes responding to temperature changes can be complicated. This is the central point of this study, namely, that changes in the *vertical distribution* of cloud amount can occur and can introduce climate feedbacks, in addition to those produced by changes in total cloud amount. As we show in the next sections, the *interaction* of vertical structure changes in total cloud amount, specific humidity and temperature produces different cloud feedbacks for different climate perturbations.

3. Sensitivity of surface temperature to solar constant increases

A commonly used measure of the sensitivity of the global surface temperature to solar constant changes is defined by (cf. Schneider and Dickinson, 1974)

$$\beta = S_0 \frac{dT_s}{dS}, \tag{12}$$

where S is the solar constant, with $S_0 = 1365$ W m^{-2} as the current value, and T_s the surface temperature. On time scales longer than one year, the earth-atmosphere system appears to be in radiative equilibrium (Jacobowitz *et al.*, 1979) and thus the outgoing thermal radiation F equals the net incoming solar radiation, $S(1 - \alpha)/4$, at the top of the atmosphere, where α is the global albedo. With this additional relationship, we can rewrite (12) to express β in terms of the thermal flux sensitivity (or greenhouse) parameter, dF/dT_s, and the albedo sensitivity parameter, $d\alpha/dT_s$:

$$\beta = F\left(\frac{dF}{dT_s} + \frac{S_0}{4}\frac{d\alpha}{dT_s}\right)^{-1}. \tag{13}$$

Since we only consider small changes in S, we will not discuss the consequent small changes in F, but concentrate on the contribution of the two sensitivity parameters to β. The effect of cloud variations on these two parameters illustrates the separate feedback effects of clouds on the solar and thermal radiative fluxes (cf. Section 2b and Fig. 1).

To study the feedbacks produced by variable clouds or temperature-dependent critical lapse rates, we must compare the climate change that results with and without each feedback. The calculation of the change in model climate without cloud or lapse rate feedback is called the control run. Although we adjust the model climate by matching the current values of global albedo and global temperature (Cess, 1976; Jacobowitz *et al.*, 1979), the control run response varies slightly because of small differences in the vertical structure (Table 1) which depends on which cloud property had been adjusted or which critical lapse rate is used. Consequently, for a proper determination of the feedback effects, we use four different control runs, one for each combination of feedbacks.

Table 2 summarizes the surface temperature changes produced by a 2% increase in the solar constant and the associated model sensitivity parameters for the control runs, labeled "no feedback", and for model runs with lapse rate feedback only, cloud feedback only, and both feedbacks. A comparison of the four control runs shows that, without cloud or lapse rate feedbacks, the model surface temperature increases by ~2.3 K for a 2% increase in the solar constant, with greenhouse and albedo parameter values of ~2.3 and −0.24 W m^{-2} K^{-1}, respectively. These values are in excellent agreement with those obtained with other 1-D RC models[5]

[5] The small negative value of the albedo parameter is caused by increasing absorption of solar radiation by water vapor which increases in abundance with increasing temperature.

TABLE 2. Effects of cloud and critical lapse rate (Γ) feedback on the surface temperature change ΔT_s (K), the thermal flux sensitivity dF/dT_s (W m^{-2} K^{-1}), the solar albedo sensitivity $(S_0/4)d\alpha/dT_s$ (W m^{-2} K^{-1}), and the model sensitivity β (K) for a 2% increase in solar constant.

Feedback	6.5 K km^{-1}				Moist adiabatic lapse rate			
	ΔT_s	$\frac{dF}{dT_s}$	$\frac{S_0}{4}\frac{d\alpha}{dT_s}$	β	ΔT_s	$\frac{dF}{dT_s}$	$\frac{S_0}{4}\frac{d\alpha}{dT_s}$	β
I. Cloud cover (A)								
1. No feedback	2.17	2.38	−0.25	109	2.28	2.25	−0.25	114
2. Γ feedback (fixed A)					1.62	3.22	−0.37	81
3. A feedback (fixed Γ)	1.95	1.57	0.78	98	1.87	1.51	0.92	93
4. (A + Γ) feedback					1.97	1.71	0.63	99
II. Cloud optical thickness (τ)								
1. No feedback	2.26	2.36	−0.24	113	2.41	2.19	−0.24	120
2. Γ feedback (fixed τ)					1.60	3.30	−0.37	80
3. τ feedback (fixed Γ)	1.95	2.20	0.25	98	1.91	2.16	0.28	95
4. (τ + Γ) feedback					1.36	3.17	0.25	68

(see Wang and Stone, 1980). This comparison also demonstrates that the model sensitivity is not dependent on the particular value of a *fixed* critical lapse rate.[6] Furthermore, this table shows that none of the feedbacks included in this model calculation is able to prevent or reverse the warming produced by a solar constant increase of this magnitude.

When the lapse-rate feedback, alone, is added to the model (labeled "Γ feedback" in Tables 2 and 3), the surface warming produced by an increased solar constant is significantly reduced; i.e., this particular temperature dependence of the lapse rate causes a negative feedback. Two opposing effects produce this result: the larger effect is an increase in surface cooling by the convective adjustment as a consequence of the decrease in the moist adiabatic lapse rate with increasing temperature, and the smaller effect is a decrease in surface cooling by infrared radiation as a consequence of the increase in downward IR flux from the relatively warmer upper atmosphere produced by the decreasing temperature lapse rate.

The latter effect is further enhanced by the presence of clouds and by fixed relative humidity. Since clouds are the only effective absorbers in the infrared spectral "window" near 10 μm, their presence decreases the IR cooling of the surface compared with clear sky conditions. Thus, a temperature-dependent lapse rate produces an additional radiative feedback on surface temperature changes even in the presence of fixed cloud cover (Ramanathan, 1977); however, the cloud contribution to this effect is only about 10–20% of the clear-sky contribution. The radiative cooling of a warming surface under clear or cloudy sky is decreased further in the model by the increase of absolute humidity at higher altitudes produced by the combination of a fixed relative humidity and a decreasing temperature lapse rate. These changes in upper level temperature and absolute humidity produced by a moist adiabatic lapse rate explain the changes in the greenhouse and albedo parameters shown in Table 2. These effects also illustrate the important point that the magnitude of any one temperature feedback in a model can depend on assumptions made regarding the vertical distribution of humidity and clouds. The interaction of even the simple parameterizations used in this model can produce rather complex behavior, as we illustrate below.

a. Variable cloud cover

When cloud cover feedback (labeled "A feedback") is added to the model, the surface warming is reduced from about 2.2 to 1.9 K, essentially independent of the value of the constant critical lapse rate used. That is, variable cloud cover produces a negative feedback. With an accompanying total cloud cover increase of 2.1% (from 50.6% for the control run), this negative feedback is largely the result of an increase in global albedo. Furthermore, the changing cloud cover now dominates the albedo sensitivity of the model climate, as shown in Table 2 by the large increase in the value of this parameter. However, Table 2 also shows that the albedo effect is partly offset by a decrease in the greenhouse parameter caused primarily by the increase in cirrus (high) cloud cover. Thus, the vertical distribution of the changes in cloud cover, shown in Fig. 2, strongly influences the magnitude of the cloud feedback. Since the cloud cover is proportional to convective heating in (10), the changes in cloud-cover vertical distribution in Fig. 2 reflect the changes in convective heating. In this case, Fig. 2 shows that the increased solar

[6] The control run for the moist adiabatic lapse rate uses a fixed critical lapse rate set equal to the moist adiabatic lapse rate calculated for the initial temperature structure.

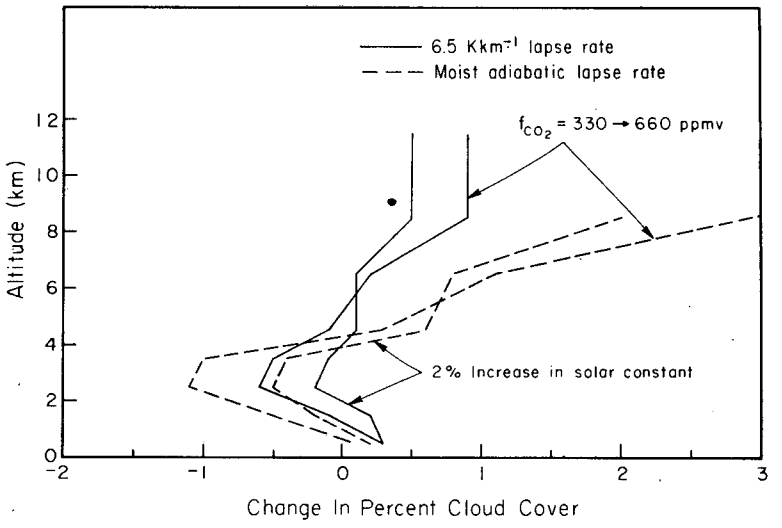

FIG. 2. Change in percent cloud fractional coverage as a function of altitude for a 2% increase in the solar constant and a doubling of the CO_2 concentration. Results are shown for models using a constant, 6.5 K km^{-1}, critical lapse rate (solid lines) and a moist adiabatic lapse rate (dashed lines) in the convective adjustment scheme.

constant causes a decrease in the heating of the atmosphere between 2 and 4 km and an increase in the heating below 2 km and in the upper troposphere above 8 km. The increase in cloud cover below 2 km is comparable to that in the upper troposphere, but the albedo effect of the optically thick, low-altitude clouds predominates over the greenhouse effect of the optically thin, high-altitude clouds.

When both the cloud-cover and lapse rate feedbacks are included (labeled "A + Γ feedback"), the surface warming is reduced with respect to the control run, but increased with respect to the Γ feedback case. That is, the cloud-cover feedback has become a positive feedback, in contrast to the case with cloud-cover feedback only. This clearly illustrates the importance of the vertical structure changes in that, even though the total cloud cover increase is larger in this case, ~2.8% (from 49% for the control run), than for the A feedback case, the greater portion of the increase occurs at higher altitudes as shown in Fig. 2. This distribution of cloud cover changes occurs because the temperature-dependent convection carries the extra solar energy primarily to higher altitudes with a stronger decrease of the heating in the 0–4 km layer. Since the optical depth of the upper level clouds is much smaller than that of the lower level clouds, the increase of the upper clouds is less important to the albedo than is the smaller decrease of lower level clouds; this accounts for the smaller albedo parameter in Table 2 for A + Γ feedback compared to that for A feedback. However, the high-level clouds significantly decrease the greenhouse parameter by blanketing the extra thermal radiation supplied by the greater convective flux from the surface. These differences from the constant lapse rate case lead to a cloud feedback of opposite sign to that produced with no lapse-rate feedback.

Paltridge (1974) constructed a model of cloud-cover feedback with solar constant changes in which all quantities are functions of the surface temperature determined from a surface energy balance including latent and sensible heat fluxes. The total cloud cover of a single-layer cloud is coupled to the latent heating of the atmosphere in a similar manner to our model. Aside from small differences in the magnitude of the change of the latent and sensible fluxes with changing solar constant produced by different formulations, these two models exhibit about the same total cloud-cover change with surface temperature and similar feedbacks on the surface temperature. However, the surface temperature change produced by a 2% increase in the solar constant is smaller in Paltridge's model because he assumes constant absolute humidity in his radiation formulation.

b. Variable cloud optical thickness

The effect of variable cloud optical thickness (labeled "τ feedback") is to reduce the surface warming from about 2.3 to 1.9 K. Although this negative feedback is coincidentally similar in strength to the A feedback case, the changes in the greenhouse and albedo parameters are smaller. The change in total cloud optical thickness of ~3.1 (from 78.65 for the control run) occurs largely in the lower altitude, optically thick clouds (Fig. 3) because of the altitude dependence of f_3; however, such increases have less effect on the albedo parameter than a change in the low-altitude cloud cover. In addition, the increase in the optical thickness of the upper level clouds begins to saturate their effect on the infrared flux

(cf. Fig. 1), so that the decrease in the greenhouse parameter is not as large as that produced by increasing the cloud cover at these altitudes.

The combined effects of lapse rate and optical thickness feedbacks (labeled "$\tau + \Gamma$ feedback") produce the largest reduction of the surface warming of any of our experiments, decreasing it from 2.4 K to about 1.4 K. This strong negative feedback occurs even though the increase in total cloud optical thickness is smaller than with τ feedback alone, in this case ~ 2.2 (from 76.39 in the control run). The larger portion of the increase occurs in the higher altitude clouds because the temperature-dependent convection transports most of the excess heat into the upper troposphere with little additional heating of the near surface atmosphere. Consequently, the upper clouds become so optically thick that their effect on the greenhouse parameter is less than their effect on the global albedo, a result which depends on the assumed initial optical thickness of these clouds in our model. These results show that substantially increasing the optical thickness of the cirrus clouds generally leads to an increasing predominance of the albedo parameter and to a more negative feedback (cf. Fig. 1), similar to the behavior of low-level clouds, and underlines the importance of correctly accounting for the behavior of cirrus clouds in climate models.

4. Sensitivity of surface temperature to CO_2 concentration increases

Table 3 summarizes the surface temperature changes produced in our model by increasing the CO_2 concentration from 330 to 660 ppmv. In the absence of cloud and lapse-rate feedbacks, doubling the CO_2 concentration causes a surface warming of ~2.1 K, in agreement with other 1-D RC model results (Ramanathan and Coakley, 1978). This amount of surface warming is comparable to that produced in our model by a 2% increase in the solar constant, but for different reasons. An increase in the solar constant directly increases the net solar heating of the surface, which is then balanced by an increase primarily of the convective cooling and secondarily of the net infrared cooling. On the other hand, increasing the CO_2 concentration decreases the net IR cooling of the surface requiring an offsetting increase of the convective cooling. Thus, the effects of these two climate perturbations on the convective heating of the atmosphere, especially its vertical distribution, are likely to be quite different and to result in different cloud feedbacks. Since adding the lapse-rate feedback, alone, only increases the relative efficiency of the convective cooling of the surface, this negative feedback is the same for a solar constant increase and a CO_2 concentration increase, as a comparison of Tables 2 and 3 shows.

a. Variable cloud cover

When cloud-cover feedback is added, the surface warming is increased from ~2–2.7 K; that is, the cloud-cover feedback is positive in contrast to the same model with a solar constant increase. The difference is caused by the vertical distribution of the cloud-cover changes, as illustrated in Fig. 2. The

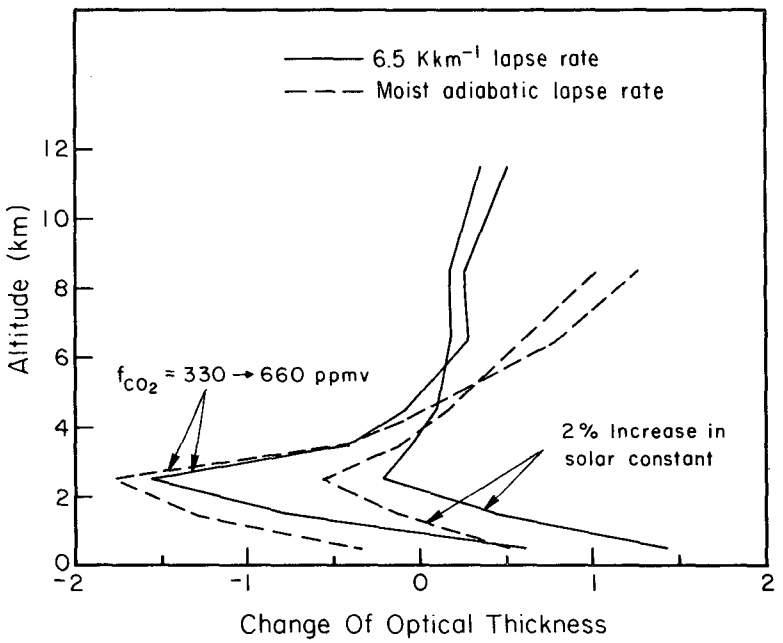

FIG. 3. Change of cloud optical thickness as a function of altitude for the same cases as in Fig. 2. Solid and dashed lines have the same meaning as in Fig. 2.

TABLE 3. Effects of cloud and critical lapse-rate feedback on the surface temperature change ΔT_s (K) due to an increase in CO_2 abundance from 330 to 660 ppmv.

	ΔT_s	
	6.5 K km^{-1}	Moist adiabatic lapse rate
I. Cloud cover (A)		
1. No feedback	1.96	2.14
2. Γ feedback (fixed A)		1.53
3. A feedback (fixed Γ)	2.68	2.62
4. (A + Γ) feedback		2.80
II. Cloud optical thickness (τ)		
1. No feedback	2.06	2.26
2. Γ feedback (fixed τ)		1.49
3. τ feedback (fixed Γ)	2.08	2.09
4. (τ + Γ) feedback		1.47

increase in the cloud cover near the surface that accompanies surface warming is the same for solar constant and CO_2 increases, but the increase in upper level clouds and decrease in middle level clouds are much larger for a CO_2 increase. Even with an increase in total cloud cover of 1.78% (from 50.6% in the control run), the global albedo has increased only slightly because more of the cloud cover increase is accounted for by the optically thin cirrus clouds than before. In addition, the large increase in the cirrus cloud cover enhances the greenhouse effect. This pattern of cloud changes is produced by the shift of the effective radiating level of the atmosphere to a higher altitude which accompanies the increase in infrared opacity with a CO_2 concentration increase; whereas, the cloud changes in response to an increase of the solar constant represent, more nearly, a simple increase in the overall atmospheric heating rate.

When both the lapse rate and cloud cover feedbacks are included, the surface warming increases to 2.8 K, larger than that in both the control run and the A feedback run; i.e., the cloud feedback is even stronger than without the lapse rate feedback, and more than offsets the negative feedback of the temperature-dependent lapse rate. Since the temperature-dependent convection produces less heating of the near-surface atmosphere and shifts the atmospheric heating to higher altitudes than the temperature-independent convection, enhancement of the cloud changes discussed above is expected (Fig. 2). Even with the larger increase of total cloud cover by 2.8% (from 49% in the control run), the larger decrease in the middle level clouds and increase in upper level clouds combine to produce the largest surface warming exhibited by any of the model calculations.

b. Variable cloud optical thickness

The optical thickness feedback produces a negligible increase in the surface warming caused by doubling the CO_2 concentration (Table 3). Fig. 3 shows that the changes in optical thickness at different altitudes nearly cancel, resulting in a total increase of only 0.1 (from 78.65 in the control run). This result depends not only on the vertical distribution of the convective heating, but also on the vertical variation of the parameter f_3 in (11). In this case, increasing the optical thickness of the upper level clouds increases the global albedo enough not only to offset the decrease in the middle-level clouds but also to reduce the relative magnitude of the greenhouse effect of these clouds (cf. Fig. 1). When the lapse-rate feedback is added, the resulting decrease in surface warming is little affected by the cloud optical thickness feedback (Table 3), despite the larger increase in the upper level cloud optical thickness. This larger increase is mostly offset by a larger decrease in middle level clouds, resulting in a total increase of only 0.47 (from 76.39 in the control run); but the albedo effect of the thicker upper level clouds now dominates their greenhouse effect, resulting in a small decrease in surface warming because of a slightly higher global albedo. This behavior of the optical thickness feedback is in sharp contrast to its behavior with solar constant increases.

5. Discussion

Most previous studies of cloud variations and feedbacks have considered only the variation of cloud cover; but even models apparently using the same cloud parameterization obtain contradictory results because of differing interactions of cloud cover with other model processes. For example, Gates (1976) and Schneider *et al.* (1978) use roughly similar prescriptions relating increasing cloud cover to increasing relative humidity; yet, in similar experiments with specified changes of fixed sea surface temperature, they found *opposite* changes of cloud cover with temperature. Comparison of these results and those from other completely different models (e.g., Temkin *et al.*, 1975; Roads, 1978) is not informative because the relationships between the clouds and other parameterized processes in these models remain unexamined. Furthermore, as our results illustrate, a simple representation of the complex behavior of clouds in one circumstance may not succeed in another situation. For example, for a doubled CO_2 concentration and a fixed critical lapse rate in our model, a shift of cloud cover from middle to upper levels is more important than the increase in total cloud cover, producing a strong positive feedback very similar to that produced by a fixed cloud temperature (FCT) parameterization in the same model (cf. Wang and Stone, 1980). However, the FCT parameterization would not reproduce the behavior of our model for a 2% solar constant increase. Thus, there is no guarantee that a cloud parameterization which is judged successful in one case will be successful for all other climate change

experiments. Consideration of the factors which control the nature of cloud feedbacks, even in simple climate models, cannot be separated from consideration of the interaction of clouds with other model processes.

One objective of many studies has been to determine the relation between the total cloud cover and the surface temperature variations. Cess (1976), for example, relates observed changes in total cloud cover with latitude and season to the observed changes in surface temperature; but he neglects the role of the varying temperature lapse rate and cloud vertical distribution. Our results illustrate the potential importance of both of these quantities; and, in particular, suggest that *total* cloud cover may not be simply related to either the surface temperature or the cloud feedbacks produced by climate variations. Several key examples of this behavior are as follows:

1) For a 2% increase of the solar constant, variable cloud cover without lapse-rate feedback reduces the surface warming by ~14% (Table 2). This small negative feedback is in contrast to the larger response obtained when the same change in total cloud cover occurs all at some specified altitude (Manabe and Wetherald, 1967; Lacis *et al.*, 1979). Our result depends on the distribution of the changes in total cloud cover in the model between changes in low-level, optically thick clouds and in high-level, optically thin clouds; an increase in the former increases the albedo more than the greenhouse effect, while an increase of the latter can increase the greenhouse effect more than the albedo (cf. Fig. 1). Thus, the vertical distribution of a cloud-cover change can influence the *magnitude* of the cloud-cover feedback on surface temperature.

2) In fact, differing vertical distributions of cloud-cover changes can change the *sign* of the cloud feedback as illustrated by comparing the differences between the no feedback and A feedback cases with the difference between the Γ feedback and $A + \Gamma$ feedback cases in Table 2.

3) Comparison of the surface temperature changes produced by a 2% solar constant increase and a doubling of the CO_2 concentration in models with cloud cover and lapse rate feedbacks (Tables 2 and 3) shows very different values for the *same total cloud-cover change* (ΔT_s = 1.97 K, ΔA = 2.81% and ΔT_s = 2.80 K, ΔA = 2.8%, respectively). Fig. 2 shows that these two cases differ only in the magnitude of the offsetting cloud-cover changes at different altitudes.

Our model results with variable cloud optical thickness show that such changes can also produce feedbacks on the surface temperature just as large as those produced by variable cloud cover (Table 2) and just as variable in sign and magnitude with differing lapse-rate assumptions and climate perturbations (Tables 2 and 3). The nature of the optical thickness feedback is sensitive to the assumed initial vertical distribution of optical thickness in the model; thus, analyses of observations to determine cloud feedbacks which assume constant cloud albedo may be in error. If both cloud cover and cloud optical thickness variations are correlated, their interaction could result in very complex cloud feedbacks on the climate.

Since the uncertainties in the global distribution of cloud properties in the current climate and the proper parameterization of the physical processes controlling it are large, we do not present our results as a proper representation of the cloud feedbacks on climate changes. Instead we present these results to *illustrate* the *potential* complexity of the cloud-feedback problem by providing an example of such complexity with a very simple climate model.

Below we summarize our conclusions:

1) The interactions between the processes controlling the vertical distribution of temperature, humidity and clouds may produce very complicated and interrelated changes in these quantities which may make the nature of cloud feedbacks dependent on the type of climate perturbation that occurs.

2) Changes in total cloud cover may not be simply related to changes of other climate variables, since variations in the vertical distribution of cloud cover without a change in the total can have equally important effects on the climate. The same may be true of the horizontal, diurnal and seasonal distributions of cloud as well.

3) Changes in other cloud properties, in particular, the optical thickness, also may play as important a role in determining the climate as fractional areal coverage.

4) Because of the complexity of behavior exhibited even by this simple model of cloud effects, conclusions about the nature of cloud feedbacks on the climate which are based on model results should be viewed with caution and require a much better understanding of model assumptions than currently exists. Much more study is required to understand the role of clouds in the climate.

Acknowledgments. We thank David Rind, Andrew Lacis and Peter Stone for many helpful conversations and useful comments on the manuscript. The Bowen ratio parameterization, used here, was suggested by Peter Stone. We thank Lilly Del Valle for the graphics. M. Wolfson was supported by NASA Cooperative Agreement NCC-5-16.

REFERENCES

Budyko, M. I., 1956: *Heat Balance of the Earth's Surface*. Gidrometeoizdat, 266 pp.

Carrier, L. W., G. A. Cato and K. L. von Essen, 1967: The backscattering and extinction of visible and infrared radiation by selected major cloud models. *Appl. Opt.*, **6**, 1209–1215.

Cess, R. D., 1974: Radiative transfer due to atmospheric water vapor: Global considerations of the earth's energy balance. *J. Quant. Spectros. Radiat. Transfer,* **14,** 861–871.

——, 1976: Climate change: An appraisal of atmospheric feedback mechanisms employing zonal climatology. *J. Atmos. Sci.,* **33,** 1831–1843.

Cox, S. K., 1971: Cirrus clouds and climate. *J. Atmos. Sci.,* **28,** 1513–1515.

Fleming, J. R., and S. K. Cox, 1974: Radiative effects of cirrus clouds. *J. Atmos. Sci.,* **31,** 2182–2188.

GARP, 1975: *The Physical Basis of Climate and Climate Modelling.* GARP Publ. Ser. No. 16, WMO, 265 pp.

Gates, W. L., 1976: The numerical simulation of ice-age climate with a global general circulation model. *J. Atmos. Sci.,* **33,** 1844–1873.

Hale, G. M., and M. R. Querry, 1973: Optical constants of water in the 200 nm to 200 μm wavelength region. *Appl. Opt.,* **12,** 555–563.

Hansen, J. E., 1971: Multiple scattering of polarized light in planetary atmospheres. Part II. Sunlight reflected by terrestrial water clouds. *J. Atmos. Sci.,* **28,** 1400–1426.

Irvine, W. M., and J. B. Pollack, 1968: Infrared optical properties of water and ice spheres. *Icarus,* **8,** 324–360.

Jacobowitz, H., W. L. Smith, H. B. Howell, F. W. Nagle and J. R. Hickey, 1979: The first 18 months of planetary radiations budget measurements from the Nimbus 6 ERB experiment. *J. Atmos. Sci.,* **36,** 501–507.

Johnson, R. H., 1980: Diagnosis of convective and mesoscale motions during Phase III of GATE. *J. Atmos. Sci.,* **37,** 733–753.

Krishnamurti, T. N., Y. Ramanathan, H.-L. Pan, R. J. Pasch and J. Molinari, 1980: Cumulus parameterization and rainfall rates I. *Mon. Wea. Rev.,* **108,** 465–472.

Lacis, A. A., and J. E. Hansen, 1974: A parameterization for the absorption of solar radiation in the earth's atmosphere. *J. Atmos. Sci.,* **31,** 118–133.

——, W. C. Wang and J. E. Hansen, 1979: Correlated k-distribution method for radiative transfer in climate models: Application to effect of cirrus clouds on climate. NASA Conf. Publ. 2076, E. R. Kreins, Ed., 309–314.

Leary, C. A., and R. A. Houze, 1980: The contribution of mesoscale motions to the mass and heat fluxes of an intense tropical convective system. *J. Atmos. Sci.,* **37,** 784–796.

Ludlam, F. H., 1980: *Clouds and Storms.* The Pennsylvania State University Press, 405 pp.

Manabe, S., and R. F. Strickler, 1964: Thermal equilibrium of the atmosphere with a convective adjustment. *J. Atmos. Sci.,* **21,** 361–385.

——, and R. T. Wetherald, 1967: Thermal equilibrium model of the atmosphere with a given distribution of relative humidity. *J. Atmos. Sci.,* **24,** 241–259.

Mason, B. J., 1971: *The Physics of Clouds.* Clarendon Press, 671 pp.

Ogura, Y., and T. Takahashi, 1971: Numerical simulation of the life cycle of a thunderstorm cell. *Mon. Wea. Rev.,* **99,** 895–911.

Oort, A. H., and E. M. Rasmussen, 1971: *Atmospheric Circulation Statistics.* NOAA Prof. Pap. No. 5, 323 pp.

Oxford, 1978: *Report of the JOC Study Conference on Parameterization of Extended Cloudiness and Radiation for Climate Models,* Oxford, 27 September–4 October 1978, WMO, 149 pp.

Paltridge, G. W., 1974: Global cloud cover and earth surface temperature. *J. Atmos. Sci.,* **31,** 1571–1576.

Petukhov, V. K., Ye. M. Feygelson, and N. I. Manuylova, 1975: The regulating role of clouds in the heat effects of anthropogenic aerosols and carbon dioxide. *Izv. Atmos. Oceanic Phys.,* **11,** 802–808.

Priestly, C. H. B., and R. J. Taylor, 1972: On the assessment of surface heat flux and evaporation using large-scale parameters. *Mon. Wea. Rev.,* **100,** 81–92.

Ramanathan, V., 1977: Interaction between ice-albedo, lapse rate and cloud-top feedbacks: An analysis of the nonlinear response of a GCM climate model. *J. Atmos. Sci.,* **34,** 1885–1897.

——, and J. A. Coakley, 1978: Climate modeling through radiative-convective models. *Rev. Geophys. Space Phys.,* **16,** 465–489.

Roads, J. O., 1978: Numerical experiments on the climate sensitivity of an atmospheric hydrologic cycle. *J. Atmos. Sci.,* **35,** 753–773.

Schneider, S. H., 1972; Cloudiness as a global climate feedback mechanism: The effects on the radiative balance and surface temperature of variations in cloudiness. *J. Atmos. Sci.,* **29,** 1413–1422.

——, and R. E. Dickinson, 1974: Climate modeling. *Rev. Geophys. Space Phys.,* **12,** 447–493.

——, W. M. Washington and R. M. Chervin, 1978: Cloudiness as a climatic feedback mechanism: Effects on cloud amounts of prescribed global and regional surface temperature changes in the NCAR GCM. *J. Atmos. Sci.,* **35,** 2207–2221.

Stephens, G. L., 1980: Radiative properties of cirrus clouds in the infrared region. *J. Atmos. Sci.,* **37,** 435–446.

——, and P. J. Webster, 1979: Sensitivity of radiative forcing to variable cloud and moisture. *J. Atmos. Sci.,* **36,** 1542–1556.

Stone, P. H., and J. H. Carlson, 1979: Atmospheric lapse rate regimes and their parameterization. *J. Atmos. Sci.,* **36,** 415–423.

Sundqvist, H., 1978: A parameterization scheme for non-convective condensation including prediction of cloud water content. *Quart. J. Roy. Meteor. Soc.,* **104,** 677–690.

Temkin, R. L., B. C. Weare and F. M. Snell, 1975: Feedback coupling of absorbed solar radiation by three model atmospheres with clouds. *J. Atmos. Sci.,* **32,** 873–880.

Wang, W. C., and P. H. Stone, 1980: Effect of ice-albedo feedback on global sensitivity in a one-dimensional radiative-convective climate model. *J. Atmos. Sci.,* **37,** 545–552.

——, Y. L. Yung, A. A. Lacis, T. Mo and J. E. Hansen, 1976: Greenhouse effects due to man-made perturbations of trace gases. *Science,* **194,** 685–690.

Webster, P. J., and G. L. Stephens, 1980: Tropical upper-tropospheric extended clouds: Inferences from winter MONEX. *J. Atmos. Sci.,* **37,** 1521–1541.

Wetherald, R. T., and S. Manabe, 1980: Cloud cover and climate sensitivity. *J. Atmos. Sci.,* **37,** 1485–1510.

Yamamoto, G., M. Tanaka and S. Asano, 1971: Radiative heat transfer in water clouds by infrared radiation. *J. Quant. Spectros. Radiative Trans.,* **11,** 697–708.